Solar Energy Materials & Solar Cells 94 (2010) 1884–1888

Contents lists available at ScienceDirect

Solar Energy Materials & Solar Cells

journal homepage: www.elsevier.com/locate/solmat

Electrical characterization of CIGSe solar cells metastability with Zn(S,O,OH)–ZnMgO interface buffer layers

J. Serhan [a], Z. Djebbour [a,b,*], A. Darga [a], D. Mencaraglia [a], N. Naghavi [c], G. Renou [c], D. Lincot [c], J.-F. Guillemeoles [c]

[a] LGEP, UMR 8507 CNRS-SUPELEC-UPMC-Univ. Paris-Sud 11, 11 rue Joliot-Curie, Plateau de Moulon, 91192 Gif-sur-Yvette Cedex, France
[b] Department of Physics and Engineering Science, University of Versailles UVSQ, 45 Av. Des Etats Unis, 78035 Versailles, France
[c] IRDEP, UMR 7174 CNRS-EDF-ENSCP, 6 Quai Watier-BP 49, 78401 Chatou Cedex, France

ARTICLE INFO

Available online 31 July 2010

Keywords:
CIGS
ZnS–ZnMgO buffer
Metastability
C–V profiling
SGP

ABSTRACT

We have studied ZnO:Al/ZnMgO/Zn(S,O,OH)/Cu(In,Ga)Se_2 solar cell (SC) metastability appearing during the measurement of its photovoltaic (PV) performances under AM 1.5 conditions, that is an increase with time of the PV parameters values before saturation, after about 20 min. These maximum values are not definitive since the SC returns to its initial state after about several hours. *C–V* profiling performed before and after the SC illumination exhibits a light soaking assisted charge redistribution within the absorber. This redistribution has been improved by thermal annealing at 200 °C. This improvement is correlated with a decrease in defects density, measured with sub-gap photocurrent.

1. Introduction

Chalcopyrite thin-film solar cells based on CIGSe absorber material have attained solar cell conversion efficiency close to 20% at laboratory scale [1]. One of the objectives in the field of CIGSe technology in the next years is to improve or at least to maintain the efficiency of these cells by replacing the classical CdS buffer layer by wider band gap and Cd free materials. With zinc-based buffer layers, prepared by chemical bath deposition (CBD), the potential to lead to high efficiencies solar cells and modules has already been demonstrated [2–5]. Recently it has been reported that using the CBD Zn(S,O,OH)/rf-ZnMgO buffer combination in CIGSe based solar cells it is possible to reach efficiency levels of 15–16% (higher than that of the reference cells with CdS, giving 14–15%) and a very high reproducibility [6,7]. However in order to reach optimal cell efficiencies post-treatments such as air annealing at 200 °C and light soaking for up to 20 min are generally needed. For industrial applications, a better understanding of the underlying mechanisms is still needed. In this work we have carried out a systematic study of metastability by performing electrical measurements before and after the post-treatments procedures. We have performed *C–V* profiling characteristics before and after the measurement of PV solar cell performances. In order to follow the metastability, the measurement of PV parameters has been carried out several times before reaching their optimal values. We have shown that these values have been enhanced by air annealing at 200 °C. In order to get a better understanding of mechanisms responsible for this enhancement, we have studied the sub-gap photocurrent (SGP) before and after this thermal annealing.

2. Experimental

CIGSe/CBD-Zn(S,O,OH)/rf-ZnMgO/ZnO:Al solar cells were prepared; the CIGSe layers were co-evaporated at Wurth Solar on glass/Mo substrates. The Zn(S,O,OH) layers were deposited by the chemical bath deposition (CBD) technique in a similar way as the CdS buffer layer [6]. The $Zn_{1-x}Mg_xO$ layers were deposited by rf magnetron sputtering using a target with $x=0.26$ [7]. Details on cells preparations are given in Refs. [6,7].

The electrical properties of cells are characterized by $J(V)$ measurements at 25 °C under illumination (AM 1.5 global spectrum, 1000 W/m^2). Typical post-treatments were thermal annealing at 200 °C for 15 min in air followed by light soaking during the solar cell performances measurements. The capacitance–voltage profiling measurements [8] were performed at high frequency, using a HP4284A precision impedance analyzer. The SGP signal was measured with the intensity modulated light at 80 Hz using a lock-in amplifier technique. The SC was illuminated with monochromatic light in the wavelength range

* Corresponding author at: LGEP, UMR 8507 CNRS-SUPELEC-UPMC-Univ. Paris-Sud 11, 11 rue Joliot-Curie, Plateau de Moulon, 91192 Gif-sur-Yvette Cedex, France. Tel.: +33 1 69 85 16 42; fax: +33 1 69 41 83 1.
E-mail address: djebbour@lgep.supelec.fr (Z. Djebbour).

0927-0248/$ - see front matter © 2010 Elsevier B.V. All rights reserved.
doi:10.1016/j.solmat.2010.07.004

800–1500 nm. The measured ac photocurrent was normalized with the ac photon flux.

3. Results and discussion

Fig. 1a shows the AM 1.5 *J–V* characteristic evolution with time till saturation of a non-thermally annealed SC. We observe that the SC starts with bad PV performances concerning the short-circuit current J_{sc} and the fill factor (FF) essentially, whose evolutions with time are plotted in Fig. 1b. Optimal values of these PV parameters are reached after about 15 min of light exposure. The salient feature is the S shape of the *J–V* curve, characteristic of a barrier strongly impeding the transport of photogenerated carriers, an effect stronger than that of a mere series resistance.

Fig. 2 shows the same characteristics as in Fig. 1, for a solar cell submitted initially to a thermal air annealing at 200 °C for up to 15 min. We note that, on one hand, the metastability affects essentially the fill factor, on the other hand, the stability is reached rapidly and the final values of PV parameters are globally improved. Indeed, we have found for the same SC that the optimal conversion efficiency varies from 10.4% for the non-annealed state to 14.7% for the annealed one. Note that J_{sc} increased significantly in the process from 25 mA/cm^2 asymptotic value to 30 mA/cm^2, and the S shape of the *I–V* curve at the initial stage of the light soaking treatment has evolved into curves characteristic of those of a large series resistance.

More than 20 solar cells of the same run have been studied, presenting an increase of J_{sc} up to 25% with thermal annealing. For both annealed and non-annealed states, modifications originating from the light soaking are reversible—the SC goes back to its initial state after one night in the dark at room temperature. Yet the changes incurred through the thermal annealing are irreversible.

For the non-annealed state we have also investigated the temperature dependence of the metastability kinetics under light soaking, by measuring the PV parameters time variation at different temperatures, starting from 200 K up to room temperature. Results for the fill factor (FF) and the conversion efficiency are shown in Fig. 3. From this figure we observe that the same saturation value of the conversion efficiency is reached after about 20 min at room temperature and after 90 min at 250 K. We also note that this improvement is nearly quenched for the lowest temperature.

In order to get better understanding of the charge redistribution under light soaking and after thermal air annealing effects on the solar cell properties, we have investigated the charge density profiles of the absorber, first, before and after light soaking and second, after thermal air annealing, by performing *C–V* profiling measurements.

Fig. 4 shows the net charge density obtained from *C–V* measurements using a standard analysis [8,9] within the absorber for three states: (i) before light soaking, (ii) after light soaking and (iii) after light soaking and air annealing. It has to be noted that this distribution, with a significant increase near the junction (i.e. at forward bias before the turn-on) and a dip slightly after the extension of the SCR is typical of chalcopyrite solar cells. From this figure we observe a high density of charge accumulation close to the buffer–absorber interface before light soaking. This accumulation, which is due to defects located next to the interface, induces a strong band bending and may allow interface recombination that could be eventually tunneling assisted (this latter point deserves however further investigations). This explains the low J_{sc} and FF values at the first time of illumination. After light soaking, we note a decrease of the accumulated charge with a charge homogenization tendency. This contributes to extend the electric field within the absorber layer and then to improve the free photogenerated charge collection.

After both thermal air annealing and light soaking, we observe a complete vanishing of the accumulated charge. The resulting profile is essentially linked to a net doping of the absorber with a quasi-uniform distribution. With this distribution, we are in the situation where the strong band bending is replaced with quasi-ideal parabolic bands, which means that there are less or no interface recombination mechanisms and then better solar cell PV performances. From quantum efficiency (QE) measurements, we could also gain some insight on the way light soaking or thermal annealing improved the solar cells. However, precise QE measurements with a good wavelength step resolution (e.g. less than 20 nm) could not be performed in this work because this necessitates more than half an hour experiment duration, during which the sample starts to return to its initial state. Nevertheless we performed rapid measurements with only a 100 nm step resolution, which show clearly that the improvement of the QE values expands on the whole spectrum taken between 400 and 1100 nm. This result shows that light soaking or annealing has not only decreased the density of recombination centres close to the interface but also that the carriers collection efficiency has been improved due to an increased space charge region width.

This result is correlated with the temperature dependence of V_{oc} as shown in Fig. 5. We have found that the ordinate intercept

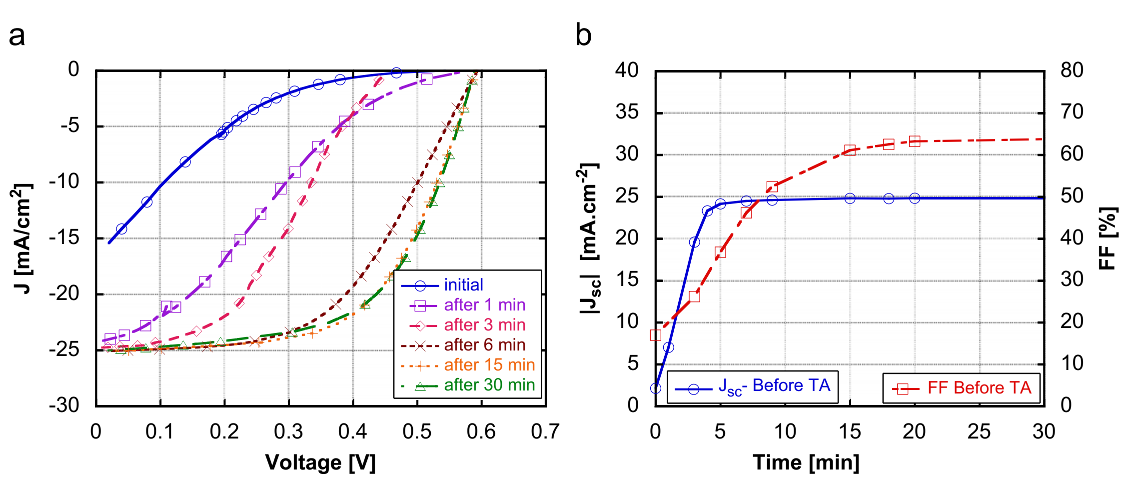

Fig. 1. AM 1.5 time dependent *J*(*V*) characteristics of a CIGSe/CBD-Zn(S,O,OH)/rf-ZnMgO/ZnO:Al solar cell (a) and time variation of the corresponding short-circuit J_{sc} current density and fill factor (FF) (b), before thermal air annealing.

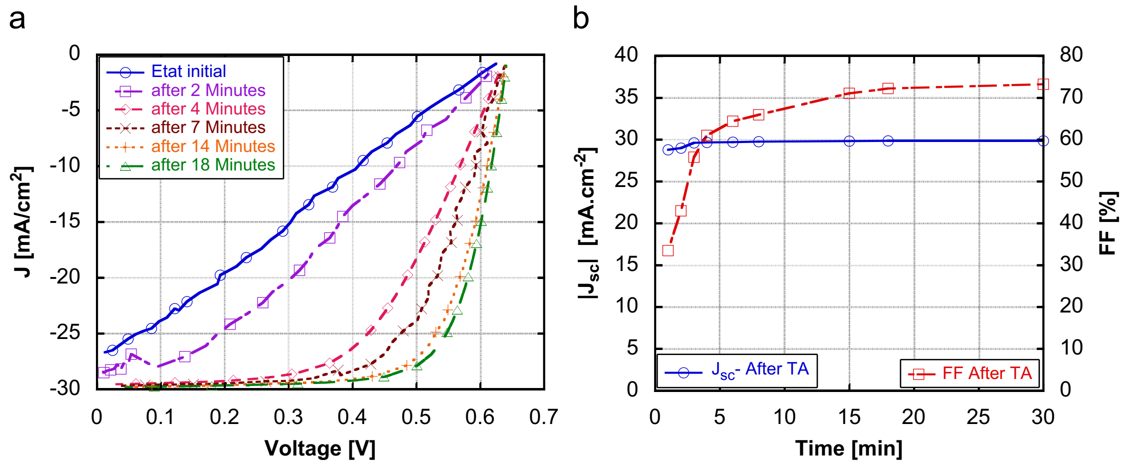

Fig. 2. AM 1.5 time dependent $J(V)$ characteristics of (a) the same solar cell as in Fig. 1 (a) and time variation of the corresponding short-circuit J_{sc} current density and fill factor FF (b), after thermal air annealing at 200 °C, during 15 min.

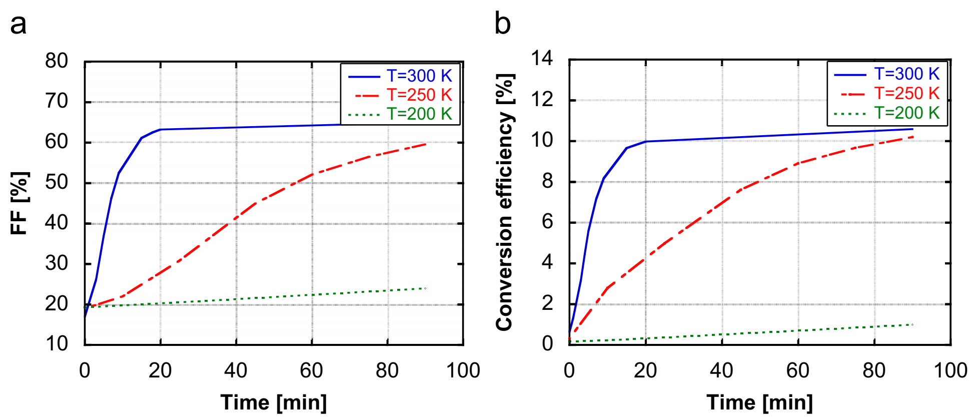

Fig. 3. Time variation under light soaking of the fill factor (a) and the conversion efficiency (b) of a non-annealed CIGSe/CBD-Zn(S,O,OH)/rf-ZnMgO/ZnO:Al solar cell, measured at AM 1.5 conditions for temperatures varying from 200 K up to room temperature.

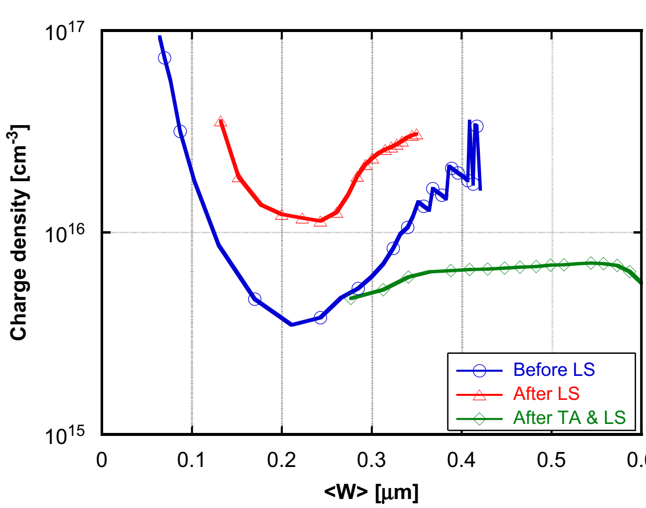

Fig. 4. Net charge density profile within the absorber of a CIGSe/CBD-Zn(S,O,OH)/rf-ZnMgO/ZnO:Al solar cell, measured for three states of the device, as explained in the text.

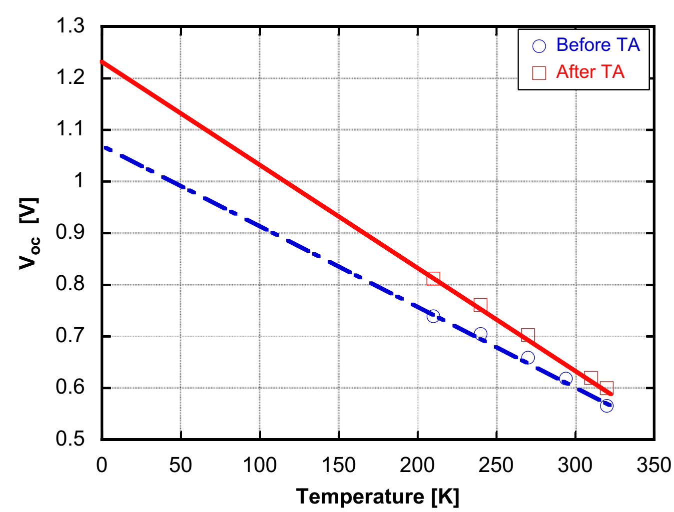

Fig. 5. Temperature dependence of the open-circuit voltage V_{oc} before and after thermal annealing at 200 °C.

is lower than the band gap of the absorber layer before annealing, and equal to the band gap after thermal air annealing followed by light soaking. Following Nadenau et al. [10], recombination mechanisms are predominant at the interface when the ordinate intercept equals the potential barrier height that is lower than the band gap value. This is the case here before thermal air annealing of our studied solar cells.

Fig. 6 shows SGP spectra for an as-deposited and thermal air-annealed solar cell. This photocurrent is a result of absorption in the absorber layer (i.e. CIGSe), since transmission results of

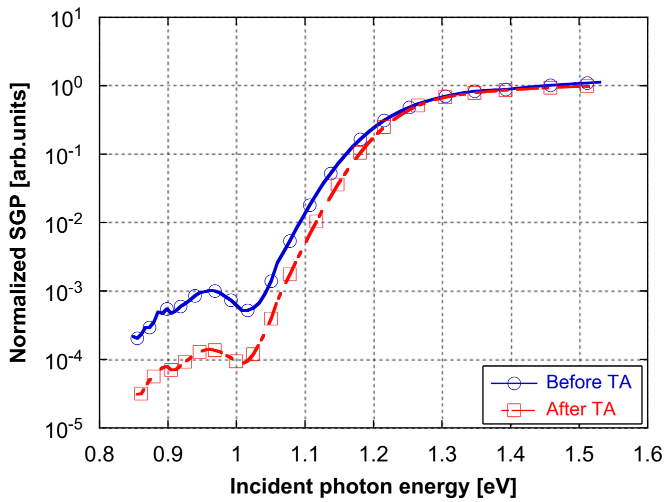

Fig. 6. Sub-gap photocurrent versus incident photon energy of solar cell before and after thermal air annealing.

window and buffer layers show no absorption for the same photon energy range. We observe the same defect absorption in both states but with a decrease of an order of magnitude between the two densities after thermal air annealing.

One explanation could be that the observed defect is linked to V_{Se}–V_{Cu} divacancies, and then the observed accumulation of negative charges next to the interface before LS may be due to the more negative charge state of these multivalent states (i.e. V_{Se}–V_{Cu} divacancies) [11–14]. These multivalent states may act as recombination centres near the junction and then enhance interface recombination mechanisms in this region. It is then clear that a diminution of the density of these vacancies will reduce the negative charge accumulation. This is what could occur by air thermal annealing.

It is noteworthy and interesting that the main effect of thermal annealing has been to greatly improve the short-circuit current and fill factor, without any significant change of V_{oc}, as shown in Fig. 2. This can help to gain more insight on the spatial location of the recombination centres that have been affected by thermal annealing. Indeed from a general and theoretical point of view, changing the space charge density somewhere in the absorber will affect the electrostatic potential difference across this layer, that is the built-in potential and consequently the open-circuit voltage. However from a practical point of view, the relative change of V_{oc} can be very small if the charge density variation is spatially located in a very thin layer. For instance, if we suppose an order of magnitude decrease of the charge density (e.g. from 10^{17} to $10^{16}\,cm^{-3}$), located in a 30 nm thick layer, one can calculate analytically or with SCAPS simulation, that the relative built-in potential variation will be around 1%, assuming a net density of charge around $10^{16}\,cm^{-3}$ across the thickness of the non-affected space charge region, the order of magnitude of which is in the micrometer range. On the contrary, the influence on short-circuit current of such a variation of the recombination centres density can be much more significant if the recombination mechanism through these centres is the predominant one. In fact the results presented in this paper, showing that short-circuit current and FF are mainly affected by thermal annealing whereas V_{oc} exhibits only very small variations, seems to indicate that the decrease of recombination centres after thermal annealing is located in a very thin layer compared with the total extent of the space charge region.

Among the prevalent models today for light induced metastability [13–16] in CdS–CIGS interfaces, one is associated with photogeneration of electrons in the absorber that modifies the equilibrium of V_{Se}–V_{Cu} divacancies and therefore the accumulation of charges near the interface. This could also be the case for Zn(O,S)/CIGS heterojunctions with more enhanced metastability in this later case due to different chemical natures of both interfaces.

Series resistance effects, with an S shape of the *J*–*V* curve, can be explained by the Zn(O,S) large CB discontinuity with CIGS, and low conductivity. About the disappearance of the S shape behavior on TA, this points out to the vanishing of the transport barrier. At this stage, the impact of TA on the very thin Zn(O,S) layer, which could easily oxidize and thus lead to a decrease of the CB discontinuity with both CIGS and ZnMgO, might be questioned. But, concerning $Zn_{1-x}Mg_xO$ with $x=0.26$, following Minemoto et al. [17], we can expect a CB discontinuity with CIGS to be around 0.3–0.4 eV. Further quantitative investigations are needed to estimate how this will be harmful or not for PV performances of our studied solar cells.

As a summary, our results are consistent with charge accumulation near the hetero interface, which degrades the internal electric field extension within the solar cell in the as-deposited state. After the device light soaking or annealing, the decrease of this accumulated charge leads to a more homogeneous space charge distribution across the absorber layer and improves by the way the electric field extension.

Finally, it should be noted that our interpretation has been given mainly as a charge redistribution in the space charge region of a homogeneous material. However, due to the grain boundaries existence typical of the polycrystalline CIGSe material, it cannot be excluded that this charge redistribution can also affect the space charge region around these grains.

4. Conclusion

The metastability of CIGSe/CBD-Zn(S,O,OH)/rf-ZnMgO/ZnO:Al solar cell has been studied by capacitance–voltage profiling and sub-gap photocurrent. *C*–*V* measurements show a redistribution of the net charge density within the absorber after the solar cell light soaking of about 20 min under AM 1.5 conditions. Thermal air annealing of the solar cell at 200 °C during 15 min shows an improvement of PV parameters, especially short-circuit current and fill factor. This improvement is correlated with a decrease of the absorber deep defect density measured by sub-gap photocurrent. The fact that thermal annealing has mainly improved the short-circuit current and the fill factor without any significant change of the open-circuit voltage can be explained by the decrease of negatively charged recombination centres located in the absorber, at the buffer/absorber interface, in a very thin layer compared with the total extent of the space charge region.

Acknowledgments

The work at IRDEP has been partly supported by the European Commission (LARCIS Contract no. FP6-19757). The authors thank N. Bouray and W. Dron for the upgrading of the sub-gap photocurrent experimental setup.

References

[1] I. Repins, M.A. Contreras, B. Egaas, C. DeHart, J. Schart, C.L. Perkins, B. To, R. Noufi, 19.9%-efficient ZnO/CdS/CuInGaSe$_2$ solar cell with 81.2% fill factor, Prog. Photovolt. Res. Appl. 16 (2008) 235–239.
[2] K. Kushiya, Development of Cu(InGa)Se$_2$-based thin-film PV modules with a Zn(O,S,OH)$_x$ buffer layer, Sol. Energy 77 (2004) 717–724.

[3] T. Nakada, M. Mizutani, Y. Hagiwara, A. Kunioka, High-efficiency Cu(In,Ga)Se_2 thin-film solar cells with a CBD-ZnS buffer layer, Sol. Energy Mater. Sol. Cells 67 (2001) 255–260.

[4] A. Ennaoui, M. Bär, J. Klaer, T. Kropp, R. Saez-Araoz, M.-Ch Lux-Steiner, Highly-efficient Cd-free $CuInS_2$ thin-film solar cells and mini-modules with Zn(S,O) buffer layers prepared by an alternative chemical bath process, Prog. Photovolt. Res. Appl. 14 (2006) 499–511.

[5] M.A. Contreras, T. Nakada, M. Hongo, A.O. Pudov, J.R. Sites, ZnO/ZnS(O,OH)/Cu(In,Ga)Se_2/Mo solar cell with 18.6% efficiency, in: Proceedings of the Third World Conference of Photovoltaic Energy Conversion, Osaka, 2003, p. 570–573.

[6] N. Naghavi, C. Hubert, O. Kerrec, D. Lincot, D. Hariskos, R. Menner, M. Powalla, Optimization studies of chemical bath deposition of Zn(S,O,OH) buffer layers for large area co-evaporated Cu(In,Ga)Se_2 and electrodeposited CuIn$(S,Se)_2$ solar cells, in: Proceedings of the 22nd EPVSEC, Milan, 2007, p. 2304–2307.

[7] D. Hariskos, D. Fuchs, M. Menner, M. Powalla, N. Naghavi, D. Lincot, The ZnS/ZnMgO buffer combination in CIGS-based solar cells, in: Proceedings of the 22nd EPVSEC, Milan, 2007, p. 1907–1910.

[8] L.C. Kimerling, Influence of deep traps on the measurement of free-carrier distributions in semiconductors by junction capacitance techniques, J. Appl. Phys. 45 (1974) 1839–1845.

[9] S.M. Sze, in: Physics of Semiconductor Devices, Wiley, New York, 1969 [9].

[10] V. Nadenau, U. Rau, A. Jasenek, H.W. Schock, Electronic properties of $CuGaSe_2$-based heterojunction solar cells. Part I. Transport analysis, J. Appl. Phys. 87 (2000) 584–593.

[11] S. Lany, A. Zunger, Light- and bias-induced metastabilities in Cu(In,Ga)Se_2 based solar cells caused by the $(V_{Se}$–$V_{Cu})$ vacancy complex, J. Appl. Phys. 100 (2006) 113725-1–113725-15.

[12] S. Lany, A. Zunger, Intrinsic DX centers in ternary chalcopyrite semiconductors, Phys. Rev. Lett. 100 (2008) 016401-1–016401-4.

[13] M. Cwil, M. Igalson, Charge and doping distributions by capacitance profiling in Cu(In,Ga)Se_2 solar cells, J. Appl. Phys. 103 (2008) 063701-1–063701-9.

[14] M. Igalson, P. Zabierowski, D. Prządo, A. Urbaniak, M. Edoff, W.N. Shafarman, Understanding defect-related issues limiting efficiency of CIGS solar cells, Sol. Energy Mater. Sol. Cells 93 (2009) 1290–1295.

[15] M. Igalson, H.W. Schock, The metastable changes of the trap spectra of $CuInSe_2$-based photovoltaic devices, J. Appl. Phys. 80 (1996) 5765–5769.

[16] P. Zabierowski, U. Rau, M. Igalson, Classification of metastabilities in the electrical characteristics of ZnO/CdS/Cu(In,Ga)Se_2 solar cells, Thin Solid Films 387 (2001) 147–150.

[17] T. Minemoto, Y. Hashimoto, T. Satoh, T. Negami, H. Takakura, Y. Hamakawa, Cu(In,Ga)Se_2 solar cells with controlled conduction band offset of window/Cu(In,Ga)Se_2 layers, J. Appl. Phys. 89 (2001) 8327.